Exploring Polarimetric Forward Operators for Use with Numerical Models

Jeffrey C. Snyder
Cooperative Institute for Mesoscale Meteorological Studies
Norman, OK

Alexander V. Ryzhkov
Cooperative Institute for Mesoscale Meteorological Studies
Norman, OK

Daniel T. Dawson
Purdue University
Norman, OK

Youngsun Jung
Center for Analysis and Prediction of Storms
Norman, OK

Alexander Khain
Hebrew University of Jerusalem
Jerusalem, Israel

Introduction and Motivation

- Significant advancements have been made in storm-scale numerical simulations and multimoment microphysics schemes that model more microphysical processes more completely.
- Polarimetric research-focused radars have been used for more than 15 years, and the amount of polarimetric weather radar data has expanded significantly over the past several years as the WSR-88D network was upgraded to dual polarization.
- Comparing radar observations with results from numerical models can be difficult since the radar does not measure the same properties that numerical models analyze or predict.
- A forward operator can be used to represent numerical model output in commonly used radar quantities, allowing one to compare observations with simulations more readily.
- Examples of polarimetric forward operators: Jung et al. (2010); Ryzhkov et al. (2011); Augros et al. (2015); Tatarevic and Kollias (2015, personal communication).

Factors to Consider

- For accurate calculation of radar quantities using a forward operator, it is generally beneficial if not necessary for the model to provide accurate information regarding the size distributions, particle densities, particle shapes, water fractions, and water distributions on mixed-phase hydrometeors.
    - Most schemes limit the shape of the size distribution (e.g., inverse exponential, gamma, etc.)
    - Most microphysics schemes currently use fixed densities for frozen species
    - Most schemes do not predict water fraction or aspect ratio
- A forward operator needs to diagnose water fraction if the model does not predict it – this can be quite challenging!
- Scattering amplitudes can be obtained from Rayleigh equations or, better, from methods that can capture resonance effects (e.g., T-matrix). Such calculations can be slow, so the use of lookup tables is common (which typically requires more assumptions to be made).
- Details such as the particle shape – size relationship, canting angle variability, and the relationship between the temperatures of water/ice and air must be specified.

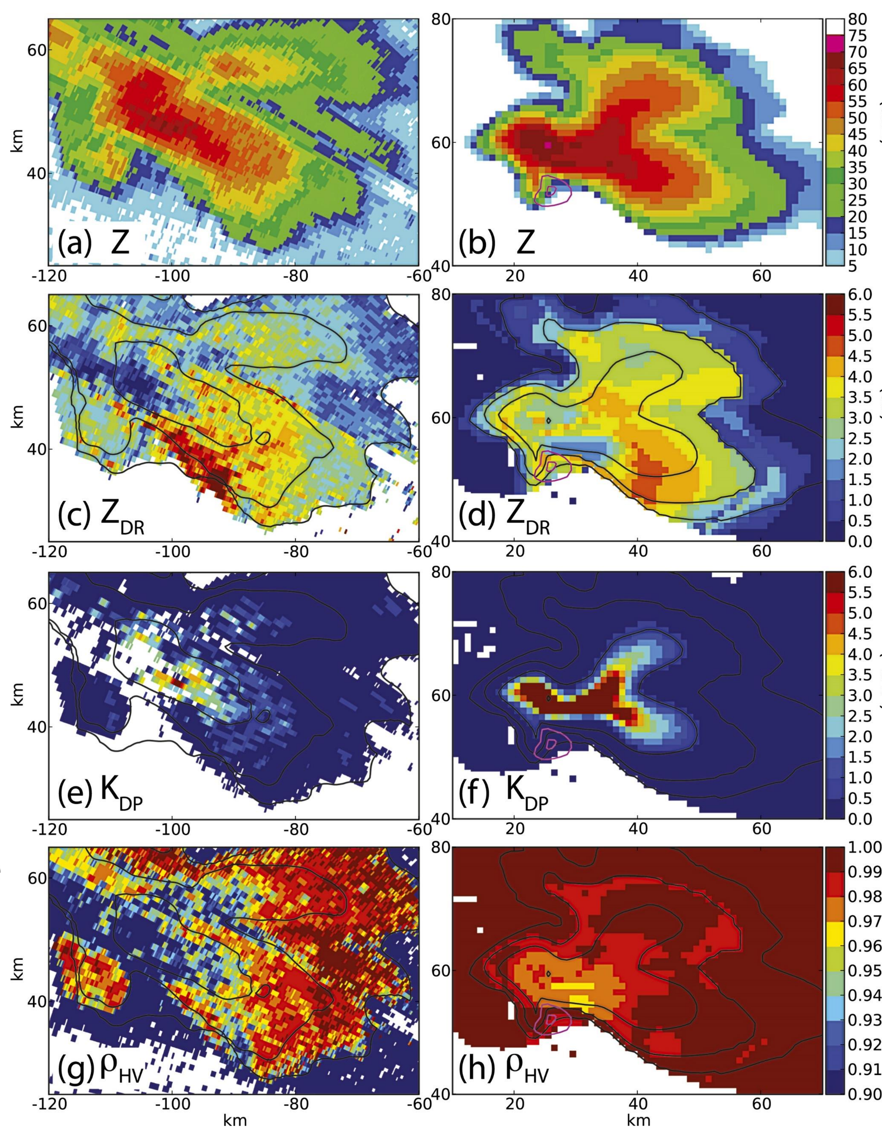

Above: (Left column) Radar observations and (right column) radar quantities from a numerical simulation of a supercell that occurred in western Oklahoma in 2008. The supercell was simulated using NSSL Collaborative Model for Multiscale Atmospheric Simulation (NCOMMAS) with a multimoment bulk microphysics scheme. These results are similar to others examined by the authors in that Z_H and Z_{DR} tend to be similar to observations, but K_{DP} and ρ_{hv} tend to be too high relative to observations. (From Dawson et al. 2014)

Radar Wavelength

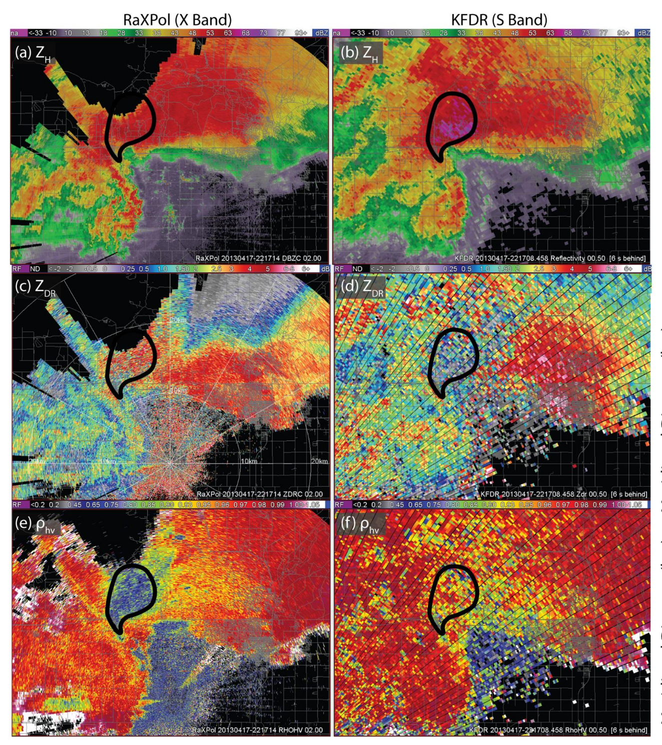

Left: Radar observations of a supercell that produced large hail in southwestern Oklahoma on 17 April 2013 as seen from RaXPol (X band) and a WSR-88D (S band).

Below: Simulated radar quantities from a high-resolution Advanced Regional Prediction System (ARPS) simulation of a supercell (Snyder 2013) processed using a forward operator based upon Jung et al. (2010).

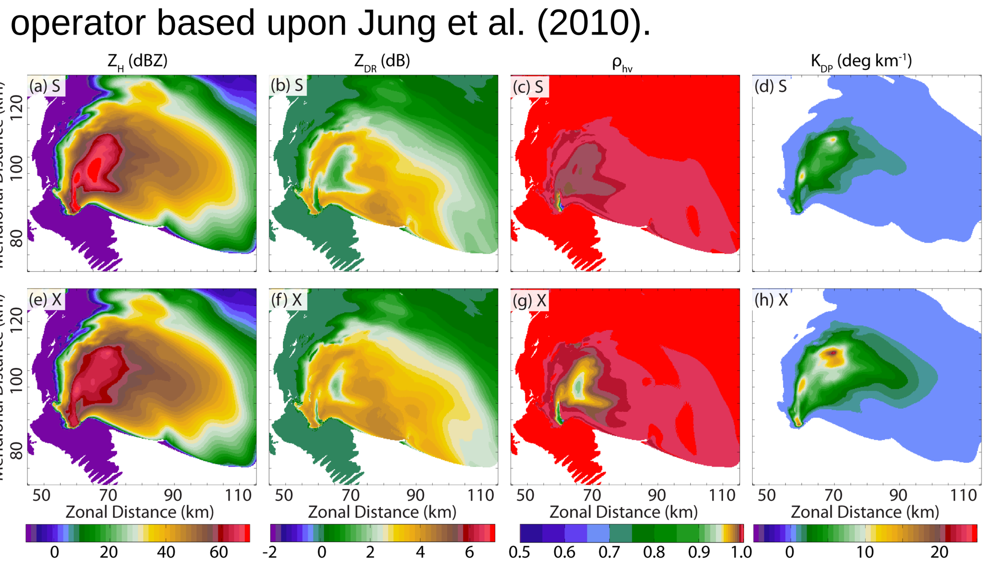

Water Fraction – Mixed-Phased Hydrometeors

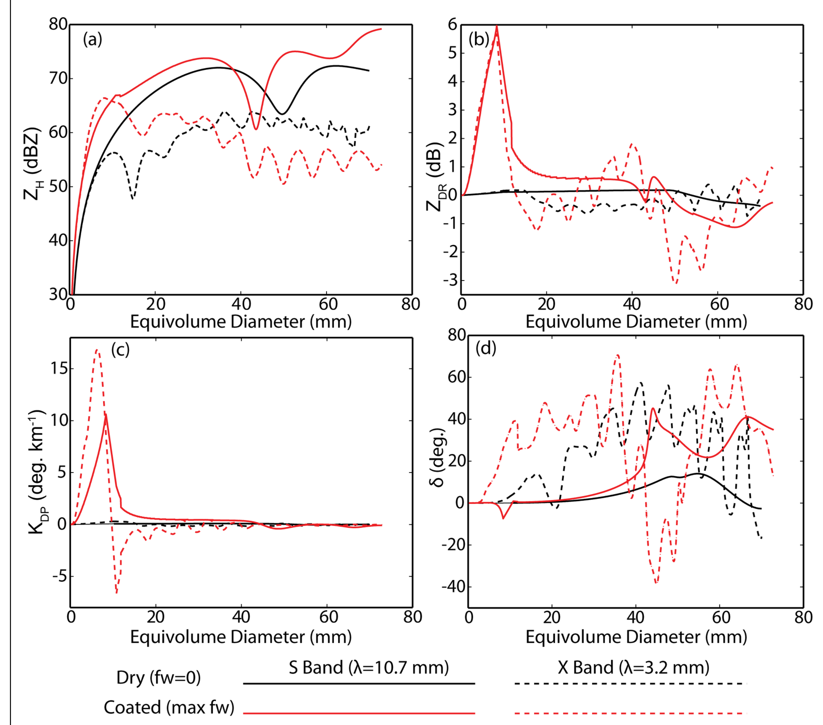

Above: Calculated radar quantities at (solid) S band and (dashed) X band valid for 2 g m^{-3} of (black) dry and (red) "wet" hail, where "wet" essentially means the hailstone has as much water as it can support without shedding (e.g., Rasmussen and Heymsfield 1987). Consequently, diameters ≤ 8 mm are raindrops; the mass water fraction varies with diameter for sizes greater than 8 mm. The hail is assumed to "tumble" as described in Jung et al. (2010).

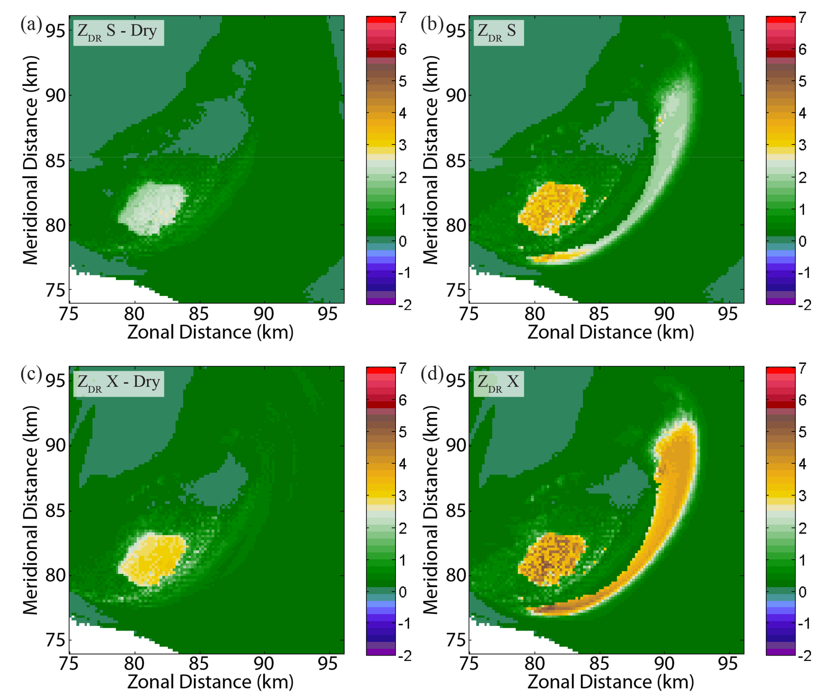

Above: ~5 km AGL Z_{DR} of a supercell simulated in ARPS at (top) S and (bottom) X bands assuming (left) no mixed-phase hydrometeors (i.e., all ice is dry) and (right) diagnosing water fraction as in Dawson et al. (2014). It can be important (electromagnetically) to simulate mixed-phased hydrometeors by diagnosing water fraction since hydrometeor composition can have a significant impact on the polarimetric quantities.

Fixed Temperature or Variable Temperature? Rayleigh Only or Include Resonance Effects?

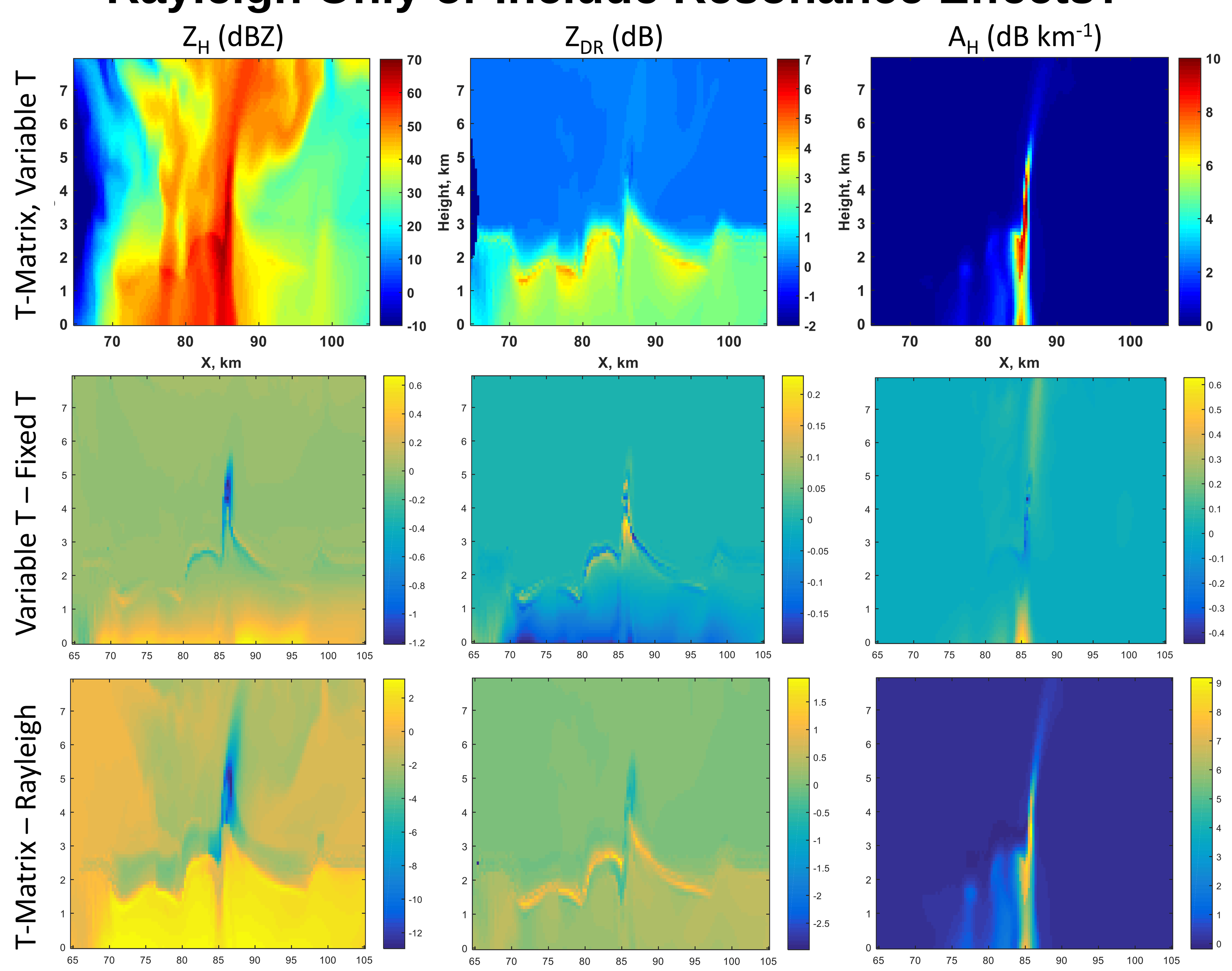

Above: (Top row) Calculated X-band Z_H, Z_{DR}, and A_H from a 2-D Hebrew University Cloud Model (HUCM) simulation with spectral bin microphysics. The dielectric constant was calculated for each hydrometeor bin at each grid point to allow the forward operator to use the temperature information from the model. (Middle row) The difference between results shown in the top row and those obtained by fixing liquid water temperature to 10 ºC and ice temperature to 0 ºC. Although fixing the temperature when calculating the dielectric constant saves computing time (since it makes it easier to create lookup tables), it does result in some errors. (Bottom row) The difference between the T-matrix results with variable temperature (i.e., top row) and the results assuming Rayleigh scattering only. The forward operator used here is based upon that from Ryzhkov et al. (2011). HUCM predicts water and rime fractions.

Mixed-Phase Water Distribution

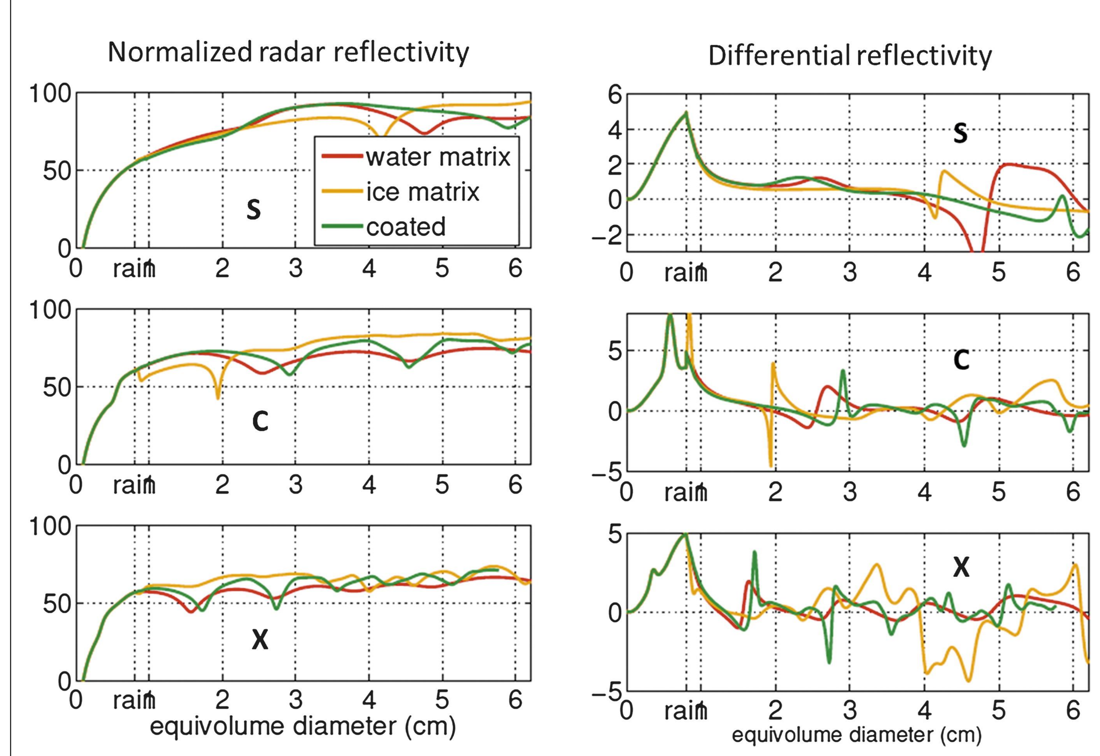

Left: Normalized (left) Z_H and (right) Z_{DR} as a function of equivolume diameter for saturated hailstones at (top row) S, (middle row) C, and (bottom row) X bands. The red and orange curves are calculated assuming a homogeneous mixture of ice and water modeled as a water matrix with ice inclusion and as an ice matrix with water inclusion, respectively. The green curve is calculated using two-layer T-matrix code. (From Ryzhkov et al. 2013)

Canting Angle Variability / Distribution

As far as we are aware, all forward operators rely upon the backscatter rule from Holt and Shepherd (1979) when accounting for canting angle variability or non-zero mean canting angles. The net result for an oblate spheroid with a mean canting angle of 0º and non-zero canting angle variance is to move the scattering amplitude in the horizontal closer to that in the vertical (and vice versa). For distributions that span abrupt changes in scattering amplitudes (i.e., where resonance effects are strong), however, this can become a source of error. For example, high canting angle variability (that is, "tumbling") for an oblate hailstone may not necessarily reduce the magnitude of the horizontal scattering amplitude relative to that from a non-tumbling hailstone. Unfortunately, there is a not a large amount of data regarding the distribution of canting angles as a function of size *and* water fraction for free-falling frozen or mixed-phased hydrometeors, particularly for those aloft.

General Comments

The results from a well-developed polarimetric forward operator will, in general, only be as good as the underlying microphysics scheme in the model. However, depending upon the intended use of the forward operator (e.g., speed vs. accuracy), the user may still have many decisions to make that can significantly affect the calculation of the radar quantities. If large hail is to be modeled, it may be important to calculate scattering amplitudes from a method other than T-matrix (e.g., see Mirkovic et al. 2015 – Poster 56). The choice of the model used for calculating the scattering amplitudes of mixed-phase or particularly large particles using the T-matrix approach (i.e., two-layer vs. homogeneous mixed-phased particle with ice or water matrix) can also be important for accurately calculating polarimetric quantities.

Acknowledgments

This poster was prepared by the first author with funding provided by NOAA/Office of Oceanic and Atmospheric Research under NOAA-University of Oklahoma Cooperative Agreement #NA11OAR4320072, U.S. Department of Commerce. The statements, findings, conclusions, and recommendations are those of the author(s) and do not necessarily reflect the views of NOAA or the U.S. Department of Commerce.

References

Augros, C., O. Caumont, V. Ducrocq, N. Gaussiat, and P. Tabary, 2015: Comparisons between S-, C-, and X-band polarimetric radar observations and convective-scale simulations of the HyMeX first special observing period. Q. J. R. Meteor. Soc., **in press**.

Dawson, D. T., E. R. Mansell, Y. Jung, L. J. Wicker, M. R. Kumjian, and M. Xue, 2013: Low-level Z_{DR} signatures in supercell forward flanks: the role of size sortin00g and melting of hail. *J. Atmos. Sci*, **71**, 276–299.

Holt, A. R., and J. W. Shepherd, 1979: Electromagnetic scattering by dielectric spheroids in the forward and backward directions. *J. Phys. A Math. Gen.,* **12,** 159–166. Jung, Y., M. Xue, and G. Zhang, 2010: Simulations of polarimetric radar signatures of a supercell storm using a two-moment bulk microphysics scheme. *J. Appl. Meteor. Climatol.*, **49**, 146–163.

Mirkovic, D., D. Zrnic, and A. V. Ryzhkov, 2015: Full wave electromagnetic approach to the calculation of polarimetric variables for ensembles of rough and nonspheroidal hydrometeors. *37th Conf. on Radar Meteor.*, Norman, OK, Amer. Meteor. Soc., 56.

Rasmussen, R. M., and A. J. Heymsfield, 1987: Melting and shedding of graupel and hail. Part I: Model physics. *J. Atmos. Sci.*, **44,** 2754–2763.

Ryzhkov, A. V., M. Pinsky, A. Pokrovsky, and A. Khain, 2011: Polarimetric radar observation operator for a cloud model with spectral microphysics. *J. Appl. Meteor. Climatol.*, **50,** 873–894.

Ryzhkov, A. V., M. R. Kumjian, and S. Ganson, 2013: Polarimetric Radar characteristics of melting hail. Part I: theoretical simulations using spectral microphysical modeling. *J. Appl. Meteor. Climatol.*, **52**, 2849–2870.

Snyder, J. C., 2013: Observations and simulations of polarimetric weather radar signatures in supercells. Ph.D. dissertation, School of Meteorology, University of Oklahoma, 213 pp.